Title
Electron microscopy of satellite tobacco mosaic virus crystals: metal-coated, negatively stained and stereo pairs.

Journal
Microscopy, 49(3)

ISSN
2050-5698

Authors
Desjardins, PR
Ban, N
Mathews, DM
et al.

Publication Date
2000

DOI
10.1093/oxfordjournals.jmicro.a023836

Journal of Electron Microscopy **(49)3**: 509–514 (2000)

Full-length paper

Electron microscopy of satellite tobacco mosaic virus crystals: metal-coated, negatively stained and stereo pairs

Paul R. Desjardins[1*], Nenad Ban[2,3], Deborah M. Mathews[1], John T. Kitasako[1,4], J. Allan Dodds[1], and Alexander McPherson[2,5]

[1]Department of Plant Pathology and [2]Department of Biochemistry, University of California, Riverside, CA 92521, USA

*To whom correspondence should be addressed

[3]Present address: Department of Molecular Biophysics and Biochemistry, Yale University, 266 Whitney Avenue, New Haven, CT 06520, USA

[4]Present address: Department of Neuroscience, University of California, Riverside, CA 92521, USA

[5]Present address: Department of Molecular Biology and Biochemistry, 3205 BS II, University of California, Irvine, CA 92697–3900, USA

Abstract Highly purified virions of satellite tobacco mosaic virus (STMV) were found to crystallize at relatively low concentrations (300–500 μg ml^{-1}) in pure water. Small crystals of these preparations were examined in the transmission electron microscope after either being rotary shadowcast with metal or negatively stained with 4% uranyl acetate. Stereo views were also obtained of both types of preparations. Stereo pairs of metal-coated crystals provided good three-dimensional images. When stereo pairs of negatively stained crystals were printed from second negatives, they provided striking images although the three-dimensional aspect was not so pronounced. Images of both types of preparations were compared with a computer-generated model of the virus. This model was based on data obtained in earlier X-ray diffraction crystallographic studies. Measurements of crystal axes on the EM images were somewhat lower than those of the computer model. It is assumed the reason for this is the dehydration of crystals during preparation for electron microscopy. The EM images did verify the type of crystal lattice determined in the X-ray diffraction studies. Conversely, knowing the exact unit cell parameters and the distribution of virions in the crystal from X-ray diffraction data aids in the further interpretation of electron micrographs of virus crystals.

Keywords satellite TMV, virus crystals, virus electron microscopy, stereo pairs, negatively stained crystals, virus crystal-computer model

Received 15 October 1999, accepted 17 January 2000

Introduction

Satellite tobacco mosaic virus (STMV) is interesting in a number of ways, one of which is the fact that it has isometric virions whereas its helper virus (TMV) has virions with helical symmetry. It has been quite well characterized biologically [1–4]. Although found naturally occurring in *Nicotiana glauca* with the U5 strain of TMV (also known as tobacco mild green mosaic virus, TMGMV) acting as the helper virus, several tobamoviruses can also serve as helper viruses [4].

In tobacco leaves co-infected with TMV and STMV, virions of the latter were found only in cells which had helper virus (TMV) virions. The STMV virions were associated with cytopathic structures that were distinct from those induced by the helper virus. One of the most striking of these structures was a crystal of STMV particles

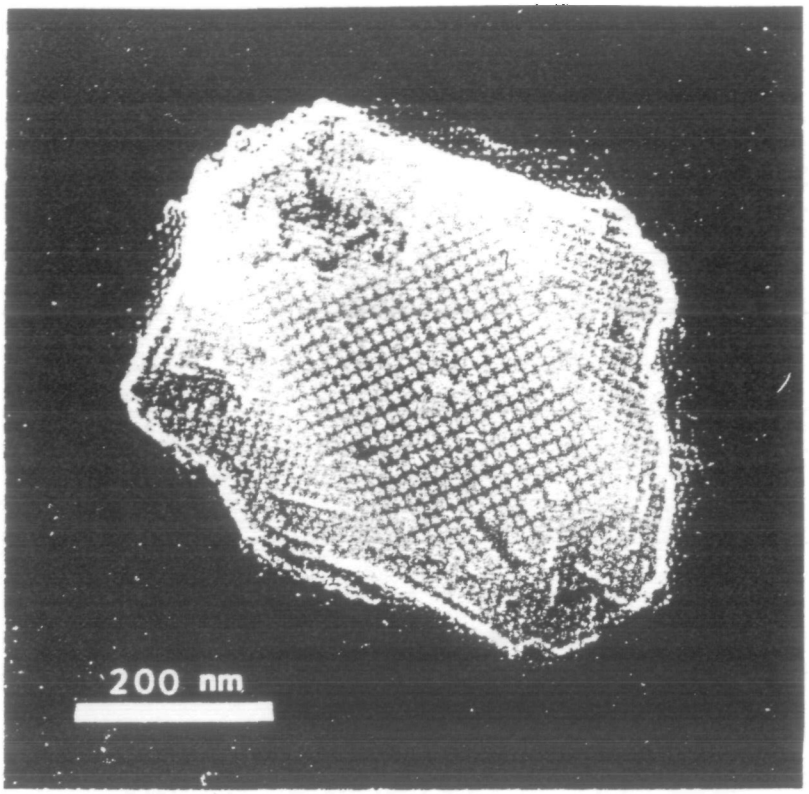

Fig. 1 Single crystal of strain 8 STMV rotary shadowcast with platinum–palladium alloy. The relatively small crystal is still in the process of formation as it is obviously not a 'complete' crystal.

which was associated with two granular inclusion bodies. Both of these structures were bound by a common membrane [5].

A number of crystallographic studies utilizing X-ray diffraction and quasi-elastic light scattering techniques have resulted in a very complete knowledge of STMV virion structure [6–9]. Laboratory produced crystals have permitted elucidation of virion structure at a 2.9 Å resolution while more perfect crystals produced in the Microgravity Laboratory have allowed a 1.8 Å resolution. Recently, a structural comparison of STMV was made with satellite tobacco necrosis virus (STNV) and satellite panicum mosaic virus (SPMV) [10]. Although the structural analysis showed a common function and the preservation of a 'jelly-roll' motif in the protein subunit for the three viruses, there were remarkable differences in the arrangement of secondary structural elements, interaction of adjacent subunits and the disposition of the subunits with respect to the icosahedral axes of symmetry. In all three viruses it was shown that the narrow end of the 'jelly-roll' forms fivefold contacts although the nature of these contacts was shown to be different for each of the three viruses. Visibility of nucleic acid in the electron density maps was found only in the case of STMV, and this was manifested as double-helical segments of RNA associated with each coat protein dimer.

The nucleotide sequence has been determined for STMV and the translation of its RNA has been accomplished [11]. Several naturally occurring isolates of STMV have been obtained from the field which differ in characteristics such as mobility of their dsRNAs [2,12] and genotype [13,14]. One of these isolates designated as strain 8, was of special interest for EM since it readily formed crystals in pure water at moderate concentrations (500 $\mu g\ ml^{-1}$). Such crystalline preparations of this strain were utilized in the present studies. Wyckoff first published electron micrographs of metal-coated virus crystals in 1949 [15]. In this report we present electron micrographs of metal-coated (rotary shadowcast) and negatively stained crystals of STMV including stereo pairs of both preparations. We also present stereo pictures of a computer model of a STMV crystal.

Methods

Virus purification

STMV (strain 8) was extracted from leaves of *Nicotiana tabacum* L. Xanthi co-infected with TMV-U5 by the purification protocol described in reference 4. However, to obtain a highly purified virus preparation, sucrose density gradient centrifugation (10–40%) was performed, fol-

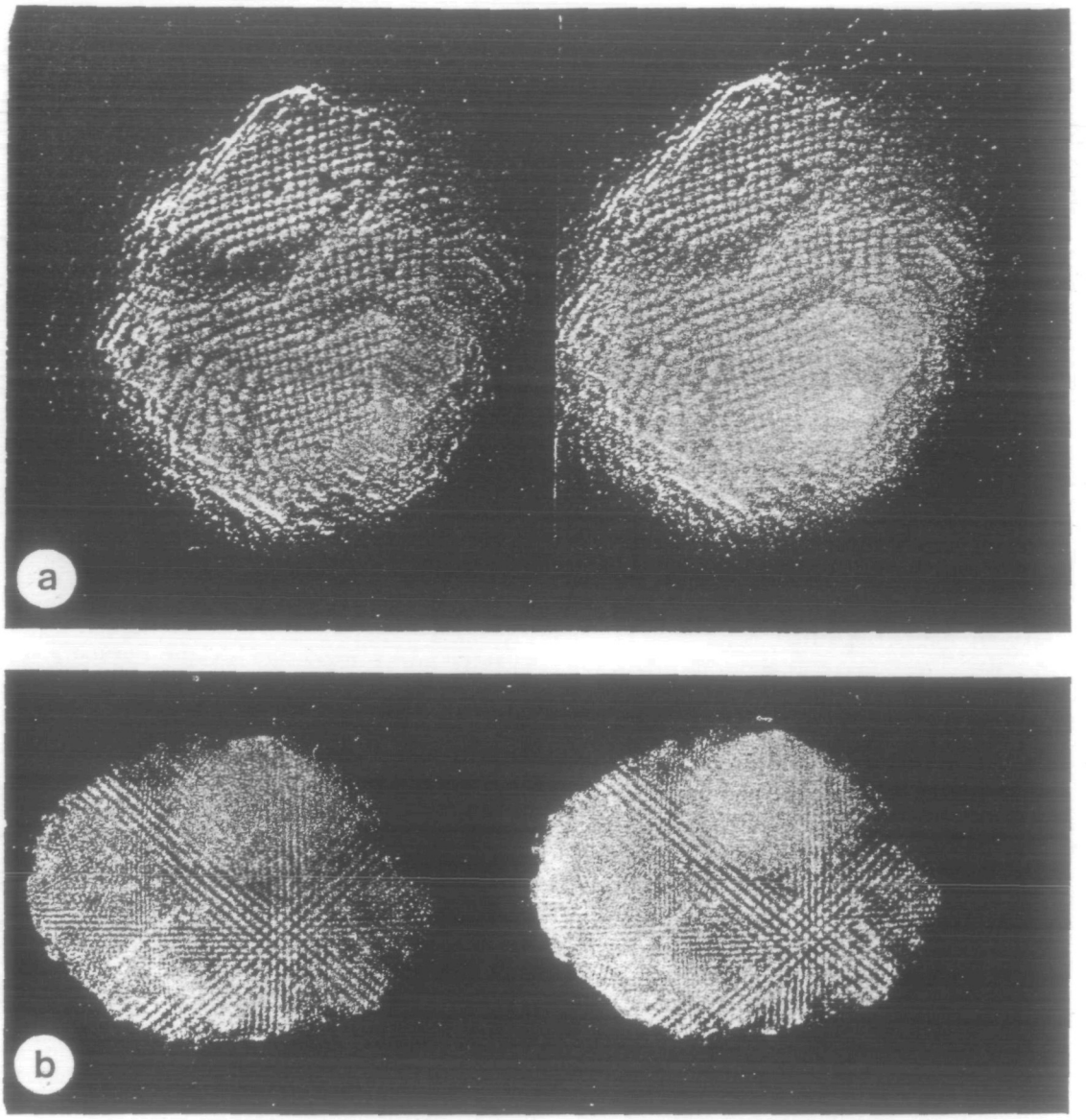

Fig. 2 Stereo pairs of electron micrographs of crystals of strain 8 STMV. (a) Single crystal rotary shadowcast with platinum–palladium alloy. (b) Single crystal negatively stained with 4% uranyl acetate. Printed from a second negative.

lowed by high speed centrifugation of the gradient fraction containing primarily STMV and the final pellet was resuspended in sterile water. This preparation was used in the electron microscope studies at concentrations of 300–500 $\mu g\ ml^{-1}$ in pure water. Since strain 8 of STMV formed crystals readily in pure water, no crystallization technique per se was used.

Electron microscope grids

Copper grids (100 mesh) with heavy carbon coated formvar films were used. The grids were exposed to a plasma glow treatment [16] shortly before use to facilitate deposition of the virus crystals which were pipetted onto the carbon coated surface of the grid. Since the STMV crystals were in pure water, it was not necessary to include a wash step before either rotary shadow casting with platinum–palladium alloy or negative staining with 4% aqueous uranyl acetate [17,18].

Electron microscope calibration

After pictures of experimental preparations were taken at a given magnification, additional pictures of a two-directional replica grating [19,20] were taken to provide a size standard. The replica grating used had 2150 lines mm^{-1} and lines were in two directions each perpendicular to the other. Use of the manufacturer's scale on the resulting photographs provided an accurate determination of the magnification.

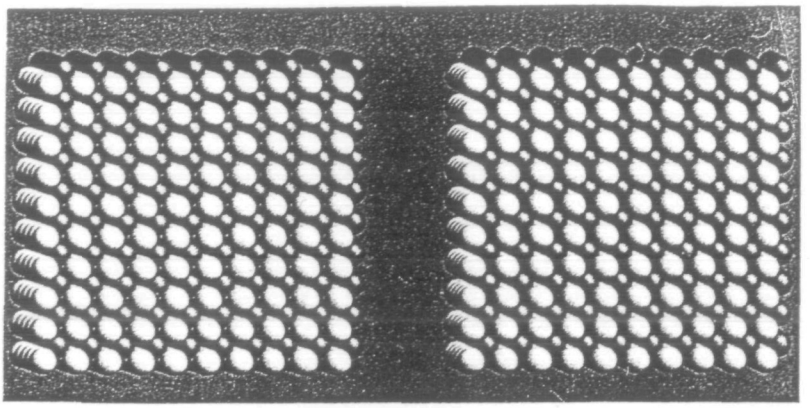

Fig. 3 Stereo schematic diagram of the packing of STMV particles in the body centred unit cell. The unit cell dimensions are a = 174.3 Å, b = 191.8 Å, and c = 202.5 Å (1 Å = 0.1 nm). There are two virus particles in the cell. This requires that the virus be centred exactly on 222 symmetry points and hence, the space group in I222. One quarter of the virus; or 15 copies of the icosahedrally related coat proteins, comprises the asymmetric unit of the crystal. Here, each virus particle is represented as a sphere. The two viral particles constituting the unit cell are shown in white and black to better demonstrate packing arrangement. The packing is viewed approximately down the c axis of the crystal lattice with the a axis being approximately horizontal. Figure was generated with RIBBONS on an SGI 320 VGX [23].

Photography of stereo pairs

The goniometer stage on the Hitachi H600 transmission electron microscope was used to obtain stereo pairs of photographs. To obtain the 'right'- and 'left'-hand views of the stereo pairs, an angle of 4° was used between the two pictures of the pair. A crystal to be photographed was first found at zero tilt of the stage. The stage was then tilted either plus 2° or minus 2°, recentred, refocused, and photographed. The stage was then tilted 2° from zero in the opposite direction (either plus or minus), the crystal recentred, refocused, and photographed. By observing the pair with a stereo viewer one could readily determine the 'right' and 'left' views of the pair [21,22].

Photography of final electron microscope images

Second negatives of pictures of metal-coated specimens are commonly utilized to give a desirable perspective view of the specimen in the final photographic print. This is obtained by making a 'contact print' of the original negative from the electron microscope onto another sheet of EM negative film. This 'second' negative is then used for the final photographic print. Pictures of negatively stained electron microscope preparations are generally printed from the original negative obtained in the microscope. However, we found that a more striking photographic image of the negatively stained crystals was obtained if a second negative was prepared. Therefore, such negatives were used for the final photographs of negatively stained virus crystals.

Computational techniques

A computer model of the STMV crystal was generated on an SGI 320 VGX workstation. A file containing coordinates for each of the virus particles in the crystal composed of 500 unit cells (10×10×5 cells) was prepared in a RIBBONS atom file format [23]. Each virion was, thus, represented as a sphere or atom. In the model, the spheres are separated according to the packing and space group parameters determined by X-ray diffraction [24].

Results and discussion

Metal-coated crystals

Large crystals, not shown, were too dense to the electron beam to permit the definition of individual virions on the surface of the crystal. The virus suspension that was deposited on the grids often had clusters of small crystals closely associated with one another. Figures 1 and 2a are of two such small crystals of STMV strain 8 which have been rotary shadow cast with a platinum–palladium alloy. These might be considered as 'incomplete' crystals as virions appear to be still depositing on the surface of the crystal. By careful observation one can note that virions in a layer below the top layer appear to be in lines that are orientated at an angle to the lines of virions in the top layer. Perhaps the virions in the lower layer are in the interior of the crystal unit cell.

Negatively stained crystals

The micrographs in Fig. 2b illustrate the images of negatively stained crystals when the photograph is printed from a second negative. Sets of white lines perpendicular to one another represent virions in one 'layer' of the crystal. The second set of white lines which are at an angle of 45° to the upper layer represent the next lower 'layer' of virions in the crystal. Since the picture was made from a second negative, one must keep in mind that the white lines are actually deposits of uranyl acetate between the rows of virions.

Stereo micrographs of crystals

The stereo pair represented in Fig. 2a (metal-coated crystal), when viewed with a stereo viewer, provides a

three-dimensional view of a crystal. An impression that virions are still being deposited on the surface of the crystal is best seen when the crystal is viewed in stereo.

The three-dimensional aspect of the stereo pair in Fig. 2a is more apparent than in the pair of a negatively stained crystal in Fig. 2b. However, the depth of the stereo image of the negatively stained preparation makes interpretation of the angles and depths between successive layers of virions easier. Stereo views of the crystals were only possible with small crystals. Replica techniques, which were not used, may have allowed for stereo images of electron dense large crystals.

Comparisons of computer model with electron micrograph images

Knowing the exact unit cell parameters and distribution of viral particles in the crystal obtained by X-ray diffraction analysis provides us with the opportunity to further interpret electron micrographs. In both metal-coated crystals and negatively stained crystals viral particles can be seen to assume regular repetitive crystalline arrangement. Furthermore, it can be seen that in every case the crystals are viewed perpendicular to one of the crystallographic faces. Since we are dealing with the body centred crystalline lattice, all particles in the second layer should be shifted with respect to the upper layer by $\frac{1}{2}$ of the crystalline period in the direction of all crystallographic axes. This arrangement is illustrated in Fig. 3. This results in a particle being positioned right in the centre and underneath each of the four particles seen in the upper layer of the crystal. This can be seen on the metal-coated electron micrographs (Figs 1 and 2a) where several single viral particles are located on the surface of the crystal. These particles always touch four of the other particles on the layer beneath. These particles appear larger since they are exposed and accumulate more metal during the coating procedure. In the case of negatively stained crystals (Fig. 2b), regular patterns can be seen. These patterns appear as four sets of intersecting parallel lines rotated approximately 45° with respect to each other. These striations can be seen as a consequence of the distribution of the virions in the crystal lattice. The particles in the crystal can be imagined to lay on rectangular nets (almost square, since the ratios of the three crystallographic axes are 1:1.1:1.2). If the space between virus particles in the crystal receives a small amount of uranyl acetate, then dense areas under the electron microscope will appear as a series of spots which will merge into lines when viewed under an angle. In a square point lattice the points can be connected with lines which are rotated by 45° with respect to each other depending on whether the points are connected along the square edge or the square diagonal (which would make the distance 1.4 times greater). In the second case the series of uranyl acetate deposits would be further apart, and lines would appear fainter. This can actually be seen in Fig. 2b, and it is schematically represented in Fig. 3.

We have carefully measured distances between viral particles as seen on electron micrographs. We have taken into account the fact that during these measurements we can only see two of the unit cell edges. The distances between viral particles could usually be correlated with the crystallographic data according to the ratios of their lengths. Systematically, the measured values have been approximately 10–15% lower than those obtained by crystallographic analysis. We presume that this is because of the evacuation and dehydration procedure employed to prepare samples on grids for electron-microscopic analysis.

The images of metal-coated crystals resemble somewhat those obtained from tobacco necrosis virus crystals and southern bean mosaic virus crystals by Wyckoff [15]. The micrographs published by Wyckoff were obtained by using the so-called pseudoreplica technique which differs from the one used in this study. A true replica technique might provide more satisfactory images since one could observe larger intact crystals.

Concluding remarks

Horne [17] used the negative stain technique to elucidate the ultrastructure of crystal lattices of a number of specimens, and he also used the technique to demonstrate the production of crystalline arrays of virus particles on the surface of carbon-coated mica support films [18]. We believe that this report is the first to utilize the negative stain technique on actual virus crystals. As stated above, the production of a second negative of images with this technique provides striking contrast between various layers of small crystals. The technique does, however, point out the great need to make every effort to avoid photographic and interpretive artifacts when applied to biological specimens as pointed out by Wergin and Pooley [25]. Although Hayat and Miller [26] have described several methods for making carbon-coated support films more hydrophilic, they did not seem to consider the plasma glow technique recommended by Jakstys [16]. We have found that the latter method provides the best hydrophilic surfaces for deposition of specimens which are to be negatively stained.

References

1 Valverde R A and Dodds J A (1986) Evidence for a satellite RNA associated naturally with the U5 strain and experimentally with the U1 strain of tobacco mosaic virus. *J. Gen. Virol.* **67**: 1875–1884.

2 Valverde R A and Dodds J A (1987) Some properties of isometric virus particles which contain the satellite RNA of tobacco mosaic virus. *J. Gen. Virol.* **68**: 965–972.

3 Dodds J A (1991) Structure and function of the genome of satellite tobacco mosaic virus. *Canadian J. Plant Pathol.* **13**: 192–195.

4 Valverde R A, Heick J A, and Dodds J A (1991) Interaction between satellite tobacco mosaic virus, helper virus, and their hosts. *Phytopathology* **81**: 99–104.

5 Kim K-S, Valverde R A, and Dodds J A (1989) Cytopathology of satellite tobacco mosaic virus crystals and its helper virus in tobacco. *J. Ultrastruct. Mol. Struct. Res.* **102:** 196–204.

6 Larson S B, Koszelak S, Day J, Greenwood A, Dodds J A, and McPherson A (1993) Double-helical RNA in satellite tobacco mosaic virus. *Nature* **361:** 179–182.

7 Larson S B, Koszelak S, Day J, Greenwood A, Dodds J A, and McPherson A (1993) Three-dimensional structure of satellite tobacco mosaic virus at 2.9 Å resolution. *J. Mol. Biol.* **231:** 375–391.

8 Malkin A J, Cheung J, and McPherson, A (1993) Crystallization of satellite tobacco mosaic virus. I. Nucleation phenomena. *J. Crystal Growth* **126:** 544–554.

9 Malkin A J and McPherson A (1993) Crystallization of satellite tobacco mosaic virus. II. Postnucleation phenomena. *J. Crystal Growth* **126:** 555–564.

10 Ban N, Larson S B, and McPherson A (1995) Structural comparison of the plant satellite viruses. *Virology* **214:** 571–583.

11 Mirkov T E, Mathews D M, DuPlessis D H, and Dodds J A (1989) Nucleotide sequence and translation of satellite tobacco mosaic virus RNA. *Virology* **170:**139–146.

12 Mathews D M and Dodds J A (1998) Naturally occurring strains of satellite tobacco mosaic virus. *Phytopathology* **88:** 514–519.

13 Kurath G, Heick J A, and Dodds J A (1993) RNase protection analyses show high genetic diversity among field isolates of satellite tobacco mosaic virus. *Virology* **194:** 414–418.

14 Kurath G and Dodds J A (1995) Mutation analysis of molecularly cloned satellite tobacco mosaic virus during serial passage in plants: Evidence for hot spots of genetic change. *RNA* **1:** 491–500.

15 Wyckoff R W G (1949) *Electron Microscopy, Technique and Applications.* (Interscience Publishing, Inc, New York.)

16 Jakstys B P (1988) Artifacts in sampling specimens for biological electron microscopy. In: *Artifacts in Biological Electron Microscopy,* eds Crang R F E and Klomparens K L, pp. 1–12, (Plenum Press, New York).

17 Horne R W (1965) The application of negative staining methods to quantitative electron microscopy. In: *Quantitative Electron Microscopy,* eds Bahr G F and Zeitler E H, pp. 316–330, (The Williams and Wilkins Company, Baltimore, MD).

18 Horne R W (1979) The formation of virus crystalline and paracrystalline arrays for electron microscopy and image analysis. *Adv. Virus Res.* **24:** 173–221.

19 Bahr G E and Zeitler E H (1965) The determination of magnification in the electron microscope. II. Means for the Determination of magnification. In: *Quantitative Electron Microscopy,* eds Bahr G F and Zeitler E H, pp. 142–153, (The Williams and Wilkins Company, Baltimore, MD).

20 Meek G A (1970) *Practical Electron Microscopy for Biologists.* (Wiley-Interscience, London.)

21 Steere R L (1972) *Stereo Electron Microscopy and Problems of Interpretation. 30th Annual Proceedings of the Electron Microscopy Society of America,* ed. Arceneaux C J, pp. 212–213, (Claitor's Publishing Division, Baton Rouge, LA).

22 Ladd M W (1973) *The Electron Microscope Handbook-Specimen Preparation and related Laboratory Procedures.* (Ladd Research Industries, Inc, Burlington, VT.)

23 Carson M (1987) Ribbon models for macromolecules. *J. Mol. Graphics* **5:** 103–106.

24 Koszelak S, Dodds J A, and McPherson A (1989) Preliminary analysis of crystals of satellite tobacco mosaic virus. *J. Mol. Biol.* **209:** 323–325.

25 Wergin W P and Pooley C C (1988) Photographic and interpretive artifacts. In: *Artifacts in Biological Electron Microscopy,* eds. Crang R F E and Klomparens K L, pp. 175–204, (Plenum Press, New York).

26 Hayat M A and Miller S E (1990) *Negative Staining.* (McGraw Hill Publishing Company, New York.)